



Empirical corrections for predicting the sound insulation of double leaf cavity stud building elements with stiffer studs

Davy, John; FARD, Mohammad; Dong, Wayland; Loverde, John

<https://researchrepository.rmit.edu.au/esploro/outputs/journalArticle/Empirical-corrections-for-predicting-the-sound/9921863589201341/filesAndLinks?index=0>

Davy, J., FARD, M., Dong, W., & Loverde, J. (2019). Empirical corrections for predicting the sound insulation of double leaf cavity stud building elements with stiffer studs. *Journal of the Acoustical Society of America*, 145(2), 703–713. <https://doi.org/10.1121/1.5089222>

Document Version: Accepted Manuscript

Published Version: <https://doi.org/10.1121/1.5089222>

Repository homepage: <https://researchrepository.rmit.edu.au>

© 2019 Acoustical Society of America.

Downloaded On 2023/12/19 15:23:43 +1100



Thank you for downloading this document from the RMIT Research Repository.

The RMIT Research Repository is an open access database showcasing the research outputs of RMIT University researchers.

RMIT Research Repository: <http://researchbank.rmit.edu.au/>

Citation:

Davy, J, Fard, M, Dong, W and Loverde, J 2019, 'Empirical corrections for predicting the sound insulation of double leaf cavity stud building elements with stiffer studs', Journal of the Acoustical Society of America, vol. 145, no. 2, pp. 703-713

See this record in the RMIT Research Repository at:

<https://researchbank.rmit.edu.au/view/rmit:51447>

Version: Accepted Manuscript

Copyright Statement:

© 2019 Acoustical Society of America

Link to Published Version:

<https://dx.doi.org/10.1121/1.5089222>

PLEASE DO NOT REMOVE THIS PAGE

1 Empirical corrections for predicting the sound insulation of double leaf cavity stud building
2 elements with stiffer studs

3
4 John L. Davy^{ab}

5
6 Mohammad Fard

7
8 Royal Melbourne Institute of Technology (RMIT) University, GPO Box 2476, Melbourne,
9 Victoria 3001, Australia

10
11 Wayland Dong

12
13 John Loverde

14
15 Veneklasen Associates, 1711 Sixteenth Street, Santa Monica, CA 90404, United States of
16 America

17
18 Running Title: Sound insulation of cavity stud elements
19

^a Author to whom correspondence should be addressed. Electronic mail: john.davy@rmit.edu.au

^b Current address: CSIRO Infrastructure Technologies, Private Bag 10, Clayton South, Victoria 3169, Australia.

20 **ABSTRACT**

21 The experimentally determined normal incident mass-air-mass resonance frequency for a double
22 leaf cavity stud building element is significantly greater than the theoretically predicted frequency
23 for wood studs and steel studs manufactured from thicker sheet steel. This paper gives a method
24 for calculating the effective mass-air-mass resonance frequency as the root mean square sum of
25 the mass-air-mass resonance frequency and the resonance frequency of the first bending wave
26 mode of the leaves between the studs. This calculation should use the isothermal mass-air-mass
27 resonance frequency if the building element cavity contains porous sound absorbing material. If
28 the cavity does not contain porous sound absorbing material, the usual adiabatic mass-air-mass
29 resonance frequency should be used in the calculation. Because the exact boundary conditions of
30 the building element leaves at the studs and the effective in situ damping are unknown, the paper
31 gives empirical correction factors to determine the actual resonance frequency and the depth of the
32 dip in the predicted sound insulation. This paper also gives empirically derived formulae for the
33 line and point equivalent translational compliances of steel studs manufactured from different
34 sheet steel gauges and compares them with formulae derived by other authors for the case of 25
35 gauge steel studs.

36

37

38

39

40 PACS numbers: 43.55.Rg, 43.55.Ti, 43.40.Rj, 43.20.Rz

41

42 **I. INTRODUCTION**

43 Theories for calculating the sound insulation of cavity stud walls predict that there will be
44 a minimum or a change of slope at the normal incidence mass-air mass resonance frequency.
45 However figure 6 in Davy (2009) with one experimental measurement for 13 mm gypsum plaster
46 board on each side of the studs, and figure 6 in Davy (2010) with three experimental measurements
47 for 16 mm gypsum plaster board on each side of the studs, both show that the dip in the measured
48 sound insulation occurs at a higher frequency than the theoretically predicted normal incidence
49 mass-air mass resonance frequency for the case of 90 mm rigid wood stud walls with porous sound
50 absorbing material in the cavity.

51 Davy (2010) comments that “Note that the predicted mass-air-mass resonance frequency
52 of about 80 Hz is significantly less than the measured mass-air-mass resonance frequencies of 125
53 or 160 Hz. This may be due to a structural resonance, which is not included in the theory described
54 in this paper. Bradley and Birta (2001) showed that the sound insulation of wood stud exterior
55 walls can be significantly degraded by a structural resonance if the two wall leaves are rigidly
56 coupled by the wooden studs. They explained this structural resonance in terms of the analysis
57 conducted by Lin and Garrelick (1977). The effects of this resonance can be reduced by structurally
58 isolating the two wall leaves with resilient mounts. The frequency of the resonance is about double
59 the calculated mass-air-mass resonance, and it reduces in frequency as the rigid stud spacing is
60 increased and as the depth of the rigid studs is increased.”

61 “Bradley and Birta (2000) reported the results of laboratory sound insulation measurements
62 on typical Canadian building facades. These measurements showed the structural resonance at 125

63 Hz. However, field measurements by Bradley *et al.* (2002) and Bradley (2002) with actual aircraft
64 noise showed little effect due to this structural resonance.”

65 Recently, Davy *et al.* (2018) also observed that the dip in the measured sound insulation
66 occurs at a higher frequency than the theoretically predicted normal incidence mass-air-mass
67 resonance frequency for cavity walls with one or two layers of 16 mm gypsum plaster board
68 screwed to both sides of steel studs made from sheet steel thicker than 25 gauge. This difference
69 in resonance frequency led to differences between the measured and predicted sound insulation of
70 up to 17.5 dB at 160 Hz. The differences between measured and predicted sound insulation in the
71 region of 160 Hz are much greater for a stud spacing of 406 mm than for a stud spacing of 610
72 mm. These observations prompted the research described in this paper.

73 The first objective of this paper is to offer a physical explanation of why the experimentally
74 observed effective mass-air-mass resonance frequency for cavity stud walls with stiffer studs is
75 significantly higher than the theoretically predicted normal incidence mass-air-mass resonance
76 frequency. The second objective is to provide formulae for the equivalent translational compliance
77 of stiffer steel studs for use in simple models for predicting the sound insulation of cavity stud
78 walls. The third objective is to point out that that the isothermal speed of sound should be used for
79 wall cavities which are filled with porous sound absorbing material. Although this paper is not
80 able to present a fully developed prediction method, because it is not able to present equations for
81 deriving some of the empirical constants, it is hoped that it will draw other researchers’ attention
82 to this important but difficult problem.

83 Van den Wyngaert *et al.* (2018) review different theories for predicting the sound insulation
84 of cavity stud walls. Lin and Garrelick (1977) is the only paper that the authors are aware of which

85 has theoretically predicted the significant increase in the effective mass-air-mass resonance
86 frequency which occurs with stiffer studs and they only considered wooden studs. Unfortunately,
87 their dimensionless variables appear to disagree with the properties of the wall whose sound
88 insulation they claimed to be calculating. Their use of the Fourier series method means that the
89 actual physical reason for the increase in effective mass-air-mass resonance frequency is not
90 obvious and they are unable to model the effects of the finite size of the wall.

91 Formulae for the equivalent translational compliance or stiffness of steel studs have only
92 been provided for 25 gauge steel studs (Poblet-Puig *et al.*, 2009; Vigran, 2010a; Davy *et al.*, 2012;
93 Hirakawa and Davy, 2015), except for a conference paper (Davy *et al.*, 2018). Narang (1993) and
94 Davy *et al.* (2017) have provided experimental evidence for the use of the isothermal speed of
95 sound in a wall cavity which is filled with sound absorbing material.

96 **II. THEORY**

97 The first bending mode between two adjacent studs of each wall leaf of a cavity stud wall
98 is modelled as a linear harmonic oscillator. These two linear harmonic oscillators are coupled by
99 the spring of the air cavity. The position, mass and stiffness of each linear harmonic oscillator are
100 x_i , m_i and K_i respectively where $i = 1, 2$. The stiffness of the spring coupling the two linear harmonic
101 oscillators is K_{12} . The system comprising the two coupled linear harmonic oscillators has kinetic
102 energy T and potential energy V . Its Lagrangian is

$$103 \quad L = T - V = m_1 \dot{x}_1^2 / 2 + m_2 \dot{x}_2^2 / 2 - K_1 x_1^2 / 2 - K_{12} (x_2 - x_1)^2 / 2 - K_2 x_2^2 / 2. \quad (1)$$

104 The Lagrangian equations of motion are

105
$$\frac{d}{dt} \left(\frac{\partial L}{\partial \dot{x}_i} \right) - \frac{\partial L}{\partial x_i} = 0 \text{ for } i = 1, 2, \quad (2)$$

106 where t is the time. Applying equations (2) to equation (1) gives

107
$$\begin{aligned} m_1 \ddot{x}_1 + (K_1 + K_{12})x_1 - K_{12}x_2 &= 0 \\ m_2 \ddot{x}_2 - K_{12}x_1 + (K_2 + K_{12})x_2 &= 0 \end{aligned} \quad (3)$$

108 To find the resonance angular frequencies of the two coupled linear harmonic oscillators,
109 assume that

110
$$x_i = a_i \exp(j\omega t) \text{ for } i = 1, 2, \quad (4)$$

111 where $a_i, i = 1, 2$, are the complex amplitudes of the two coupled linear harmonic oscillators and ω
112 is the angular frequency. This assumption gives

113
$$\begin{pmatrix} K_1 + K_{12} - \omega^2 m_1 & -K_{12} \\ -K_{12} & K_2 + K_{12} - \omega^2 m_2 \end{pmatrix} \begin{pmatrix} a_1 \\ a_2 \end{pmatrix} = \begin{pmatrix} 0 \\ 0 \end{pmatrix}. \quad (5)$$

114 Equation (5) can only be true for non-zero $a_i, i = 1, 2$, if the determinant of the matrix in
115 equation (5) is zero. Thus

116
$$(K_1 + K_{12} - \omega^2 m_1)(K_2 + K_{12} - \omega^2 m_2) - K_{12}^2 = 0. \quad (6)$$

117 Dividing equation (6) by $m_1 m_2$ gives

118
$$(K_1/m_1 + K_{12}/m_1 - \omega^2)(K_2/m_2 + K_{12}/m_2 - \omega^2) - (K_{12}/m_1)(K_{12}/m_2) = 0. \quad (7)$$

119 Putting

120
$$f = \frac{\omega}{2\pi}, f_1 = \frac{1}{2\pi} \sqrt{\frac{K_1}{m_1}}, f_2 = \frac{1}{2\pi} \sqrt{\frac{K_2}{m_2}}, f_{a1} = \frac{1}{2\pi} \sqrt{\frac{K_{12}}{m_1}} \text{ and } f_{a2} = \frac{1}{2\pi} \sqrt{\frac{K_{12}}{m_2}}, \quad (8)$$

121 gives

122
$$(f^2 - f_1^2 - f_{a1}^2)(f^2 - f_2^2 - f_{a2}^2) - f_{a1}^2 f_{a2}^2 = 0. \quad (9)$$

123 Expanding this equation gives

124
$$f^4 + pf^2 + q = 0, \quad (10)$$

125 where

126
$$p = -(f_1^2 + f_2^2 + f_{a1}^2 + f_{a2}^2) \text{ and } q = f_1^2 f_2^2 + f_1^2 f_{a2}^2 + f_2^2 f_{a1}^2. \quad (11)$$

127 Thus, the resonance frequencies of the system comprising two coupled linear harmonic
128 oscillators are

129
$$f_{\pm} = \sqrt{(-p \pm \sqrt{p^2 - 4q})/2}. \quad (12)$$

130 If $f_1 = f_2 = f_0$ and $f_{a1} = f_{a2} = f_a$ then equation (9) becomes

131
$$(f^2 - f_0^2)(f^2 - [f_0^2 + 2f_a^2]) = 0, \quad (13)$$

132 and its positive solutions give the two resonance frequencies of the coupled linear harmonic
133 oscillators as

134
$$f_- = f_0 \text{ and } f_+ = \sqrt{f_0^2 + 2f_a^2}. \quad (14)$$

135 In the situation considered in this paper, the frequency f_i is the resonance frequency of the
 136 first bending mode of the i th wall leaf between two adjacent studs and f_{ai} is the normal incidence
 137 mass-air resonance frequency of the i th wall leaf and the air in the wall cavity.

138 The normal incidence mass-air resonance frequency f_{ai} of the i th wall leaf and the air in the
 139 wall cavity is

$$140 \quad f_{ai} = \frac{1}{2\pi} \sqrt{\frac{\rho_0 c^2}{dm_i}}, \quad (15)$$

141 where ρ_0 is the density of air, m_i is the mass per unit area of the i th wall leaf, d is the width of the
 142 wall cavity and c is the speed of sound in air. This means that if $m = m_1 = m_2$ is the mass per unit
 143 area of each wall leaf, the second term under the square root in equation (14) is the square of the
 144 normal incidence mass-air-mass resonance frequency f_{mam} .

$$145 \quad \sqrt{2f_a^2} = \frac{1}{2\pi} \sqrt{\frac{\rho_0 c^2 (m+m)}{d mm}} = \frac{1}{2\pi} \sqrt{\frac{\rho_0 c^2 (m_1+m_2)}{d m_1 m_2}} = f_{mam}, \quad (16)$$

146 Thus, when the wall leaves are the same, the lower resonance frequency f_- is the resonance
 147 frequency of the first bending mode of a wall leaf between two adjacent studs and the higher
 148 resonance frequency f_+ is the root mean square sum of f_0 and f_{mam} . The situation is more
 149 complicated when the two wall leaves are different, and the resonance frequencies are given by
 150 equation (12).

151 The frequency f_i is the resonance frequency of the first bending mode of the i th wall leaf
 152 between two adjacent studs. The problem is that the exact boundary conditions at the studs are not

153 known. If the boundary conditions were simply supported at each stud or guided at each stud, the
 154 resonance frequency f_i of the first bending mode of the i th wall leaf between two adjacent studs is

$$155 \quad f_i = \frac{\pi}{2L^2} \sqrt{\frac{E_i h_i^2}{12\rho_i(1-\nu_i^2)}}, \quad (17)$$

156 where L is the spacing between the studs and E_i , ν_i , ρ_i and h_i are respectively the Young's modulus,
 157 the Poisson ratio, the density and the thickness of the i th wall leaf. Note that

$$158 \quad m_i = \rho_i h_i \quad (18)$$

159 On the other hand, if the boundary conditions were clamped at each stud or free at each
 160 stud

$$161 \quad f_i = \frac{3.56}{L^2} \sqrt{\frac{E_i h_i^2}{12\rho_i(1-\nu_i^2)}} \quad (19)$$

162 Equation (19) produces resonance frequency values which are 2.27 times greater than those
 163 given by equation (17). Because the wall leaves are vibrating out of phase in the effective mass-
 164 air-mass resonance mode, a rigid stud line connection will stop the wall leaves from moving at the
 165 line connection. Because the vibration of a wall leaf is symmetrical about the stud line connection
 166 in the effective mass-air-mass resonance mode, the part of the wall leaf on one side of the line
 167 connection will stop the part of the same wall leaf on the other side rotating at the line connection.
 168 Thus, the boundary conditions are likely to be close to clamped. As the studs become less rigid,
 169 the boundary conditions, imposed by the studs and the wall leaves on the other sides of the studs,
 170 are expected to depart further from clamped boundary conditions. Nightingale and Bosmans
 171 (1999) have shown experimentally that point connections of a building leaf to a stud behave like

172 line connections when their spacing is less than half the bending wave length of the building leaf.
173 Thus, the above conclusions for line connections also apply to point connections in the low
174 frequency region where the effective mass-air-mass resonance occurs. As the spacing between the
175 point connections becomes greater than half the bending wavelength of the building leaf with
176 increasing frequency, the behaviour of point connections gradually starts to differ from the
177 behaviour of a line connection.

178 In this paper, the resonance frequency of the first bending mode between the studs is
179 calculated by multiplying equation (17) for the simply supported resonance frequency by an
180 empirical correction factor r . Japanese researchers (Masuda and Tanaka, 2018) use a similar
181 approach to calculate the resonance frequencies of concrete floor slabs by multiplying the
182 approximate formula for the resonance frequencies of a clamped panel by a frequency multiplier.
183 The empirical correction factor r is determined by choosing the value which gives the best
184 agreement between theory and experiment. It will be greater than zero and is expected to be less
185 than 2.27. Unfortunately, this empirical correction factor r does vary between the different types
186 of wall construction examined in this paper. An important output of this research is the value of
187 this empirical correction factor r for a range of different wall constructions.

188 Because the vibration of the two wall leaves in the mass-air-mass resonance mode is out
189 of phase there will be a surface through the studs where the studs are stationary. This means that
190 the studs will not transmit any translational energy. Because the vibration of a wall leaf in the
191 mass-air-mass resonance mode is symmetrical about the effective line connection between the stud
192 and the wall leaf, the wall leaf will not rotate at the connection to the stud and hence will not
193 transmit rotational energy. This conclusion applies regardless of the stiffness of the studs. This
194 means that the leaves are effectively not coupled by the studs when vibrating in the mass-air-mass

195 resonance mode. Of course, the studs will transmit power for other types of leaf motion by coupling
196 the motion of the wall leaves.

197 The critical frequency f_{ci} of the i th building element leaf is

$$198 \quad f_{ci} = \frac{c^2}{2\pi} \sqrt{\frac{12\rho_i(1-\nu_i^2)}{E_i h_i^2}} \quad (20)$$

199 The experimental observation is that a building leaf consisting of two layers, which
200 individually have same sheet material properties and thickness, and which is screwed or spot glued
201 to the studs, has the same critical frequency as a single layer with the same sheet material properties
202 and thickness. The reason is that the spot fastening enables the two layers to slide relative to each
203 other when bent dynamically, provided the bending wave length is shorter than the screw spacing.
204 In the sound insulation prediction method used in this paper, this behaviour is modelled by treating
205 the double layers as a single layer with twice the thickness and one quarter of the Young's modulus
206 of the actual single layer sheets. This means that the product $E_i h_i^2$ is the same for both the double
207 layer and single layer building element leaves. Thus, these double and single layer leaves have the
208 same critical frequencies and the same bending wave resonances between studs with the same
209 spacing.

210 The theory used to predict the sound insulation of cavity stud building elements in this
211 paper is that of Davy (2009; 2010; 2012). This theory uses the cavity width and the mass per unit
212 area of each building element leaf to calculate the adiabatic mass-air-mass resonance frequency.
213 In order to replace this frequency with the upper resonance frequency f_+ , the adiabatic mass-air-
214 mass resonance frequency equation (the last two expressions in equation (16)) is inverted and used

215 to calculate the equivalent cavity width d_{eq} which would make the adiabatic mass-air-mass
216 resonance frequency equal to the upper resonance frequency f_+ .

$$217 \quad d_{eq} = \rho_0 \frac{m_1 + m_2}{m_1 m_2} \left(\frac{c}{2\pi f_+} \right)^2 \quad (21)$$

218 This equivalent cavity width is used instead of the actual cavity width when applying the existing
219 theory of Davy (2009; 2010; 2012) in order to avoid reprogramming the existing theory.

220 All the cavity stud walls considered in this paper had porous sound absorbing material in
221 their wall cavities. The effect of the porous sound absorbing material in the cavity is modelled as
222 the sound absorption coefficient of the cavity sides of the wall leaves following the approach of
223 Mulholland *et al.* (1967). Based on the observations of Narang (1993) and Davy *et al.* (2017) that
224 adding porous sound absorbing material to a wall cavity changes the speed of sound from the
225 adiabatic value to the isothermal value, the isothermal speed of sound was used in equation (15).
226 Note however that the adiabatic speed of sound is used in equation (21). For 25 gauge studs, it
227 appears experimentally that the decrease due to the isothermal speed of sound in wall cavities filled
228 with sound absorbing material counteracts the smaller increase in the mass-air-mass resonance
229 frequency due to the drum mode.

230 One difference from Davy (2009), is that because all the wall cavities of the walls
231 considered in this paper contain sound absorbing material, the sound absorption coefficient α of
232 the wall cavity is set equal to the maximum value given by equation (35) of Davy (2009). However,
233 because the theory could not predict some of the very deep dips in the sound insulation spectrum
234 at the upper resonance frequency f_+ , in some cases the sound absorption coefficient of the wall
235 cavity is multiplied by a factor B at and below a frequency f_B . The empirical values B and f_B are

236 determined by making the theory agree with experiment as well as possible. The values of this
237 factor B and the upper frequency f_B at which it is used are important outputs of this paper.

$$238 \quad \alpha = \begin{cases} Dkd_{eq} & \text{if } kd_{eq} < 1 \\ D & \text{if } kd_{eq} \geq 1 \end{cases} \quad (22)$$

$$239 \quad D = \begin{cases} B & \text{if } f \leq f_B \\ 1 & \text{if } f > f_B \end{cases} \quad (23)$$

$$240 \quad 0 < B \leq 1 \quad (24)$$

241 k is the wavenumber of sound in air. Another difference from Davy (2010) and Davy (2012) is that
242 sound transmission between the wall leaves via the studs is included below the resonance
243 frequency.

244 **A. Review of Davy's sound insulation theory**

245 The sound insulation theory used in this paper (Davy, 2009; Davy, 2010; Davy, 2012)
246 assumes that the sound transmission via the air in the wall cavity and the sound transmission via
247 the studs can be predicted separately and added together to obtain the actual sound transmission.
248 Both wall leaves and the air cavity are assumed to be of infinite lateral extent.

249 For sound transmission via the air cavity, the studs are assumed to have no effect on the air
250 cavity or on the vibration and sound radiation of the wall leaves. This assumption works well
251 because the reduction of the airborne induced vibration of the wall leaves caused by the studs
252 appears to be cancelled out by the increase in radiation efficiency due to the presence of the studs.
253 Only the forced vibration of the wall leaves is included when calculating the radiated sound power

254 below the critical frequency due to the airborne induced vibration because the radiation efficiency
255 of the resonant vibration is so much lower.

256 Below $2/3$ of the mass-air-mass resonance frequency, the sound insulation of the wall is
257 modelled as though it is a single leaf wall with the same total mass per unit area. The angular
258 dependent mass law is integrated over angle of incidence up to a frequency and size dependent
259 limiting angle to account for the effect of the actual finite size of the panel on the radiation
260 efficiency (Sewell, 1970).

261 Between the mass-air-mass resonance frequency and the critical frequency, the angular
262 dependent air borne sound transmission via the cavity is calculated using equation (C-10) of
263 Rudder (1985) which is derived using the approach of Mulholland *et al.* (1967). This equation
264 models the sound absorption in the cavity as a sound absorption coefficient of the cavity sides of
265 the wall leaves. This equation is approximated by assuming that its value is that which occurs at
266 the oblique mass-air-mass resonance angle of incidence. This assumption is fine when the wall
267 cavity contains sound absorbing material. For an empty wall cavity, a sound absorption coefficient
268 which is greater than the actual physical sound absorption coefficient of the wall leaves needs to
269 be used to counteract the effects of this assumption. The angular dependent air borne sound
270 transmission is integrated up to the maximum of Sewell's (1970) variable limiting angle and 61.4° .
271 The 61.4° is chosen to make the theory agree with Sharp's (Sharp, 1973; 1978; Sharp *et al.*, 1980)
272 theory. At low frequencies, the cavity sound absorption coefficient is limited as indicated in
273 equations (22) to (24). The sound transmission via the wall cavity between $2/3$ of the mass-air-
274 mass resonance frequency and the mass-air-mass resonance frequency is calculated by
275 interpolation.

276 When the frequency is greater than the lower of the critical frequencies of the two wall
277 leaves, a method similar to that used by Cremer (1942) is followed. This approach assumes that
278 most of the sound transmission occurs at angles of incidence close to the coincidence angle and
279 that the critical frequencies are not too different. It extends Cremer's method by only integrating
280 over angles of incidence from 0 to 90 degrees rather than extending the limits to plus and minus
281 infinity in order to make integration easier as Cremer did. It also uses the resonant radiation
282 impedance for a finite size panel rather than that for an infinite size panel. This resonant radiation
283 impedance is set equal to one above the lower of the critical frequencies of the two wall leaves.
284 Between 0.9 times and 1 times the lower of the two critical frequencies the resonant radiation
285 impedance is interpolated. Below the critical frequency, the maximum resonant transmission is
286 assumed to occur at grazing angles of incidence, and the resonant transmission predicted by this
287 approach is combined with the forced transmission predicted as described above to model the
288 increase of sound transmission as the critical frequency is approached from below

289 The stud borne sound transmission of the cavity wall is modelled using Heckl's (1959a; b)
290 theory for sound radiation of a panel due to point and line excitation. For line connections, it is
291 assumed that all the vibration propagation in the wall leaves is normal to the line connections. The
292 theory differs from Sharp's theory (Sharp, 1973; 1978; Sharp *et al.*, 1980) by integrating over the
293 angle of incidence of the exciting diffuse field sound instead of dividing the mass per unit area of
294 the wall leaves by 1.9, and by replacing Sharp's empirical correction factor of 5 dB with the effects
295 of the resonant vibration of the wall leaves. This paper also extends the theory to frequencies at
296 and above the critical frequencies of the wall leaves and allows the connections to be modelled as
297 four pole networks. It differs from Vigran's theory (2010a; b) by assuming that the frequency is
298 small compared to the critical frequency when calculating the radiation of an infinite version of

299 the second wall leaf due to the structural connection acting on it and correcting for this by including
300 the resonant radiation of the finite version of the wall leaf. The resonant radiation efficiency is
301 limited to a maximum value of one. Wood studs are assumed to be rigid and massless. Steel studs
302 are assumed to be massless translational springs whose stiffness varies with frequency. The line
303 connection theory is asymmetrical with regard to the critical frequencies and the damping loss
304 factors of the wall leaves. This is partially solved by requiring the calculation to be made in the
305 direction from the wall leaf with the lower critical frequency towards the wall leaf with the higher
306 critical frequency. However, as Heckl pointed out in a personal communication with the first
307 author, it is still asymmetrical with regard to the damping loss factors of the wall leaves. This is
308 solved by using the average of the damping loss factors for both wall leaves.

309 **III. THE EQUIVALENT TRANSLATIONAL COMPLIANCE OF STEEL** 310 **STUDS**

311 The equivalent translational compliance of a steel stud frame and the method that fastens the
312 wall leaves to the steel stud frame is the compliance of translational line springs spaced at the stud
313 spacing distance for the line connection model, or the compliance of translational point springs for
314 the point connection model, which transfer the same amount of vibrational power between the two
315 wall leaves as the steel stud frame and the method that fastens the wall leaves to the steel stud
316 frame. The number of translational point springs per unit area is equal to the number of connections
317 per unit area between the steel stud frame and a wall leaf. The equivalent translation compliance
318 for the line connection model has dimensions of length per (force per unit length) giving
319 dimensions of length squared per unit force or the inverse of pressure. For the point connection
320 model, the dimensions of the equivalent translational compliance are length per unit force. The
321 power transmitted by the actual steel stud frame between the wall leaves can be transmitted by

322 both translational motion and rotational motion.

323 This section gives the equivalent translational compliance of 92 mm deep C-section steel
324 studs empirically derived by Davy *et al.* (2018) for use in sound insulation prediction models. The
325 equivalent translational compliance C_M is a function of the frequency f , the number of point
326 connections per unit area n or the stud spacing b , the reduced surface density m_r , the sheet
327 steel gauge g and the area S of the test wall. The reduced surface density is

$$328 \quad m_r = \frac{m_1 m_2}{m_1 + m_2}. \quad (25)$$

329 TABLE I. The thickness in mm of different gauges of sheet steel according to different authors.

Gauge g	Dong and Loveerde (2015)	Quirt <i>et al.</i> (1995)	Poblet-Puig <i>et al.</i> (2009)	Nash (2006)
26		0.45 mm		0.551 mm
25	0.41 mm	0.53 mm	0.47 mm	0.6274 mm
20 equivalent	0.58 mm			
20	0.91 mm			
18	1.17 mm	1.22 mm		
16	1.45 mm	1.52 mm		

330

331 It is used because it is how the two surface densities are combined in the equation used to calculate
332 the normal incidence mass-air-mass resonance frequency of the cavity wall. The thickness in mm
333 of different gauges of sheet steel according to different authors is given in TABLE I. The actual
334 measured thickness in mm of the steel studs in the walls which are analysed in this paper are those

335 in the second column of TABLE I. It should be noted that there is quite a range of thicknesses in
 336 mm for a given gauge in TABLE I, especially for the thinner higher gauge number sheet steel. The
 337 20 gauge equivalent studs are made from steel thinner than 20 gauge, and are marketed by the
 338 manufacturer as having the same strength and other structural properties as 20 gauge studs.

339 TABLE II. Values and confidence limits for the constants in the low and high frequency range
 340 for the line connection model.

Frequency Range	Constant	Value	95% Upper limit	95% Lower limit
63 to 250 Hz	A (1/Pa)	6.07×10^{-4}	2.67×10^{-3}	1.38×10^{-4}
	x_f	-1.040	-0.903	-1.178
	x_m	-1.40	-1.16	-1.65
	x_g	0.666	1.084	0.249
250 to 5000 Hz	A (1/Pa)	2.58×10^{-4}	4.38×10^{-4}	1.52×10^{-4}
	x_f	-1.52	-1.49	-1.54
	x_m	-1.12	-1.03	-1.21
	x_b	-0.257	-0.134	-0.379
	x_g	1.52	1.67	1.37

341

342 The empirical equations for the equivalent translational compliance C_M are

343
$$C_M = A \left(\frac{f}{f_0} \right)^{x_f} \left(\frac{m_r}{m_{r0}} \right)^{x_m} \left(\frac{b}{b_0} \right)^{x_b} \left(\frac{g}{g_0} \right)^{x_g} \left(\frac{S}{S_0} \right)^{x_s} \quad \text{(Line connection)} \quad (26)$$

344 and

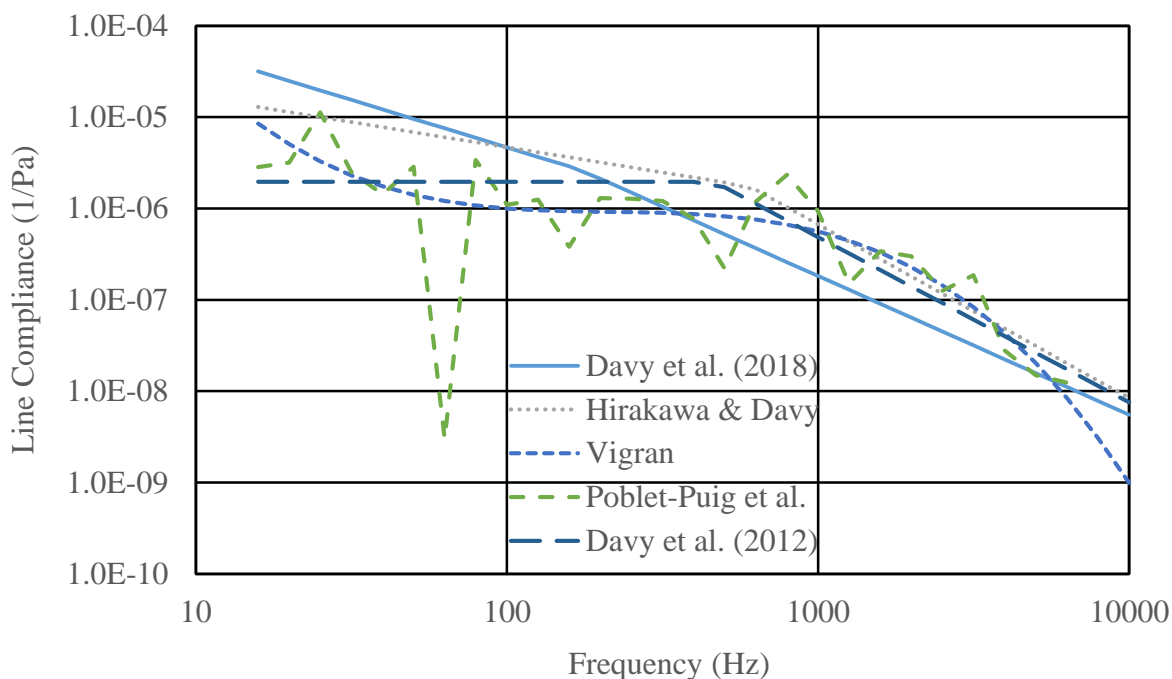
345
$$C_M = A \left(\frac{f}{f_0} \right)^{x_f} \left(\frac{m_r}{m_{r0}} \right)^{x_m} \left(\frac{n}{n_0} \right)^{x_n} \left(\frac{g}{g_0} \right)^{x_g} \left(\frac{S}{S_0} \right)^{x_S} \text{ (Point connection)}. \quad (27)$$

346 TABLE III. Values and confidence limits for the constants in the low and high frequency range
 347 for the point connection model.

Frequency Range	Constant	Value	95% Upper limit	95% Lower limit
63 to 250 Hz	A (m/N)	4.06×10^{-5}	7.11×10^{-4}	2.32×10^{-6}
	x_f	-0.760	-0.493	-1.026
	x_m	-1.96	-1.48	-2.44
	x_g	1.68	2.49	0.64
250 to 5000 Hz	A (m/N)	4.94×10^{-7}	2.15×10^{-6}	1.14×10^{-7}
	x_f	-1.16	-1.10	-1.21
	x_m	-1.18	-0.97	-1.39
	x_n	0.747	1.042	0.452
	x_g	2.49	2.87	2.11
	x_S	0.355	0.550	0.159

348
 349 A is a constant, f is the frequency, f_0 is 1 Hz, m_r is the reduced surface density, m_{r0} is 1
 350 kg/m², b is the distance between the line connections (stud spacing), b_0 is 1 m, n is the number of
 351 point connections per unit area calculated from the stud spacing and the screw spacing, n_0 is 1
 352 1/m², g is the gauge of the sheet steel used to manufacture the steel studs, g_0 is 1, S is the area of
 353 the wall and S_0 is 1 m². The constant A has units of 1/Pa for line connections and m/N for point
 354 connections. The symbols x_f , x_m , x_g , x_S , x_b , or x_n are dimensionless exponent constants. The values

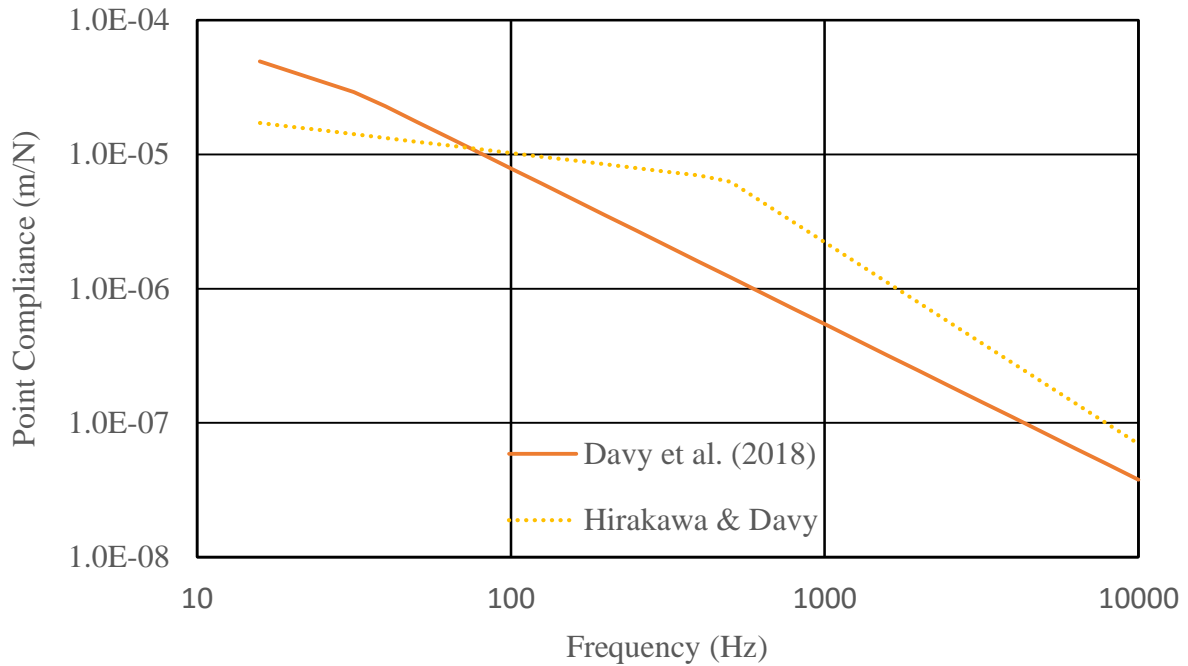
355 and 95% confidence limits of A and the dimensionless exponent constants are given in TABLE II
 356 for the line connection model and in TABLE III for the point connection model. If a dimensionless
 357 exponent constant does not appear in the applicable Table for a particular frequency range and
 358 model, the factor involving it is not used for that particular frequency range and model.



359
 360 FIG. 1. (Color online) The line compliance of nominal 25 gauge steel studs, with gypsum plaster
 361 board leaves with a reduced surface density of 4.9 kg/m^2 , a stud spacing of 0.6 m and a stud
 362 width of 70 mm, derived by Davy et al. (2018), Hirakawa and Davy (2015), Vigran (2010a),
 363 Poblet-Puig et al. (2009) and Davy et al. (2012).

364 FIG. 1 compares the line compliance of nominal 25 gauge steel studs, with gypsum plaster
 365 board leaves with a reduced surface density of 4.9 kg/m^2 , a stud spacing of 0.6 m and a stud width
 366 of 70 mm, derived by Davy et al. (2018) with that derived by Hirakawa and Davy (2015), Vigran
 367 (2010a), Poblet-Puig et al. (2009) and Davy et al. (2012). FIG. 2 compares the point compliance
 368 of nominal 25 gauge steel studs, with gypsum plaster board leaves with a reduced surface density

369 of 4.9 kg/m^2 , with 5.4 point connections per square metre and a specimen area of 7.4 m^2 . derived
 370 by Davy et al. (2018) with that derived by Hirakawa and Davy (2015). There is rough agreement
 371 between these compliances derived by different authors.



372
 373 FIG. 2. (Color online) The point compliance of nominal 25 gauge steel studs, with gypsum
 374 plaster board leaves with a reduced surface density of 4.9 kg/m^2 , with 5.4 point connections per
 375 square metre and a specimen area of 7.4 m^2 derived by Davy et al. (2018) with that derived by
 376 Hirakawa and Davy (2015).

377 IV. RESULTS

378 The empirically determined bending wave resonance frequency multiplier and sound
 379 absorption coefficient multiplier for 92 mm steel stud cavity walls, with layers of 16 mm gypsum
 380 plaster board (GPB) on each side, measuring 3.66 m wide by 4.57 m high are given in Table IV.

381 Table IV. Empirically determined bending wave resonance frequency multiplier and sound
 382 absorption coefficient multiplier for 92 mm steel stud cavity walls, with layers of 16 mm gypsum
 383 plaster board (GPB) on each side, measuring 3.66 m wide by 4.57 m high. The maximum
 384 frequency for the application of the sound absorption multiplier is also given.

Gauge g	Spacing b (m)	GPB Layers	GPB Layers	Frequency Multiplier r	Absorption Multiplier B	Upper Frequency f_B (Hz)
16	0.4064	2	2	1.7	0.4	160
16	0.4064	2	1	1.7	0.4	160
16	0.4064	1	1	1.7	0.4	160
16	0.6096	2	2	1.7	1	0
16	0.6096	2	1	1.7	1	0
16	0.6096	1	1	1.7	1	0
18	0.4064	2	2	1.3	0.5	160
18	0.4064	2	1	1.3	0.5	160
18	0.4064	1	1	1.3	0.7	160
18	0.6096	2	2	1.7	1	0
18	0.6096	2	1	1.7	1	0
18	0.6096	1	1	1.3	1	0
20	0.4064	2	2	1.3	0.5	160
20	0.4064	2	1	1.3	0.6	160
20	0.4064	1	1	1.3	0.6	160
20	0.6096	2	2	1.7	1	0
20	0.6096	2	1	1.7	1	0
20	0.6096	1	1	1.7	1	0
20E	0.4064	2	2	1.3	1	0
20E	0.4064	2	1	1.3	1	0
20E	0.4064	1	1	1.3	1	0
20E	0.6096	2	2	1.7	1	0
20E	0.6096	2	1	1.7	1	0
20E	0.6096	1	1	1.3	1	0
25	0.4064	2	2	1	1	0
25	0.4064	2	1	1	1	0
25	0.4064	1	1	1	1	0
25	0.6096	2	2	1	0.6	80
25	0.6096	2	1	1	0.6	80
25	0.6096	1	1	1	0.15	63

385

386 Table V. Empirically determined bending wave resonance frequency multiplier and sound
 387 absorption coefficient multiplier for 92 mm steel stud cavity walls, with layers of 16 mm gypsum
 388 plaster board (GPB) on each side, measuring 3.66 m wide by 2.44 m high. The maximum
 389 frequency for the application of the sound absorption multiplier is also given.

Gauge g	Spacing b (m)	GPB Layers	GPB Layers	Frequency Multiplier r	Absorption Multiplier B	Upper Frequency f_B (Hz)
16	0.4064	2	2	1.3	0.7	160
16	0.4064	2	1	1.3	0.7	160
16	0.4064	1	1	1.3	0.7	160
16	0.6096	2	2	1.7	0.5	80
16	0.6096	2	1	1.3	0.5	80
16	0.6096	1	1	1.3	0.5	80
20	0.4064	2	2	1.3	0.6	160
20	0.4064	2	1	1.3	0.6	160
20	0.4064	1	1	1.3	0.6	160
20	0.6096	2	2	1.7	0.6	100
20	0.6096	2	1	1.3	0.6	100
20	0.6096	1	1	1.3	0.6	80
25	0.4064	2	2	0.8	1	0
25	0.4064	2	1	0.6	0.8	125
25	0.4064	1	1	0.6	0.8	125
25	0.6096	2	2	0.6	0.4	80
25	0.6096	2	1	0.6	0.6	80
25	0.6096	1	1	0.6	0.6	80

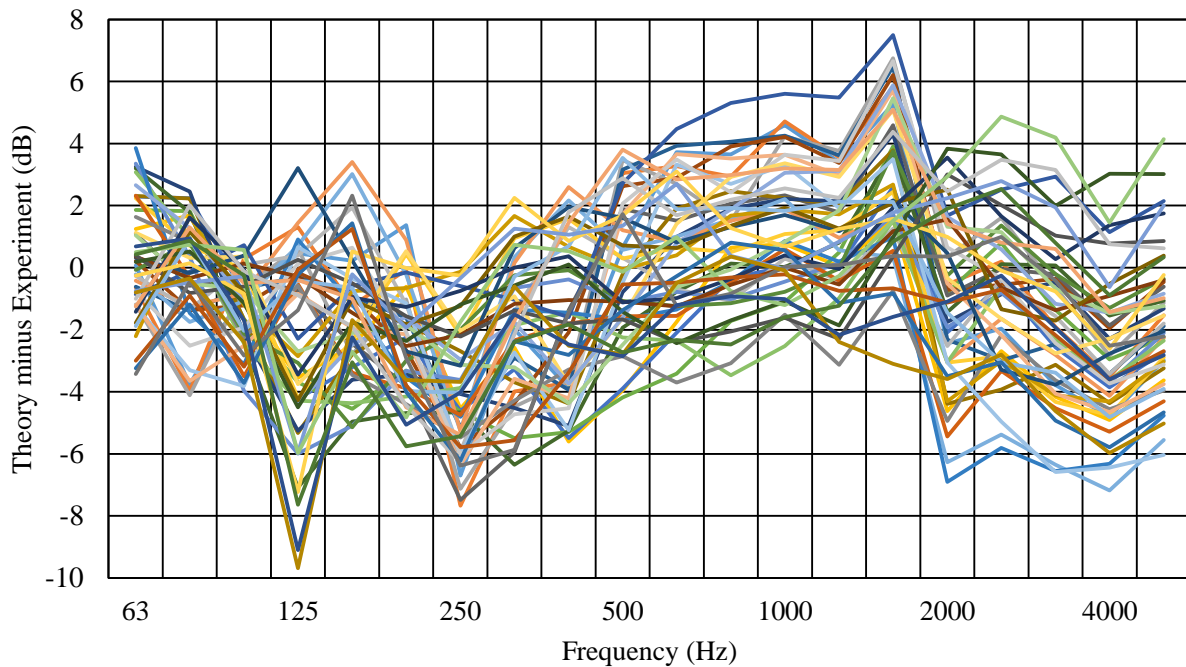
390 The maximum frequency for the application of the sound absorption multiplier is also given
 391 in Table IV. The same information for 92 mm steel stud cavity walls measuring 3.66 m wide by
 392 2.44 m high is given in Table V. The steel stud wall data is taken from B  tit (2010), Loverde et al.
 393 (2012) and Dong and Loverde. (2015). This is the same data that was used to derive the steel stud
 394 line and point compliances given in section III.

395 Table VI. Empirically determined bending wave resonance frequency multiplier and sound
 396 absorption coefficient multiplier for 39 x 89 mm wood stud cavity walls, with layers of 13 or 16
 397 mm gypsum plaster board (GPB) on each side, measuring 3.05 m wide by 2.44 m high. The
 398 maximum frequency for the application of the sound absorption multiplier is also given. The
 399 numbers in the GPB Layers columns denote the thicknesses of the GPB layers in mm. The letter
 400 X denotes type X fire rated GPB.

GPB Layers	GPB Layers	Frequency Multiplier r	Absorption Multiplier B	Upper Frequency f_B (Hz)
13X	13X	1.9	0.3	160
13	13	1.5	0.3	125
13X	13X	1.7	0.3	125
16X	16X	1.4	0.3	160
13X	13X+13X	1.7	0.3	160
13	13+13	1.7	0.2	125
16X	16X+16X	1.5	0.3	160
13X+13X	13X+13X	1.7	0.3	160

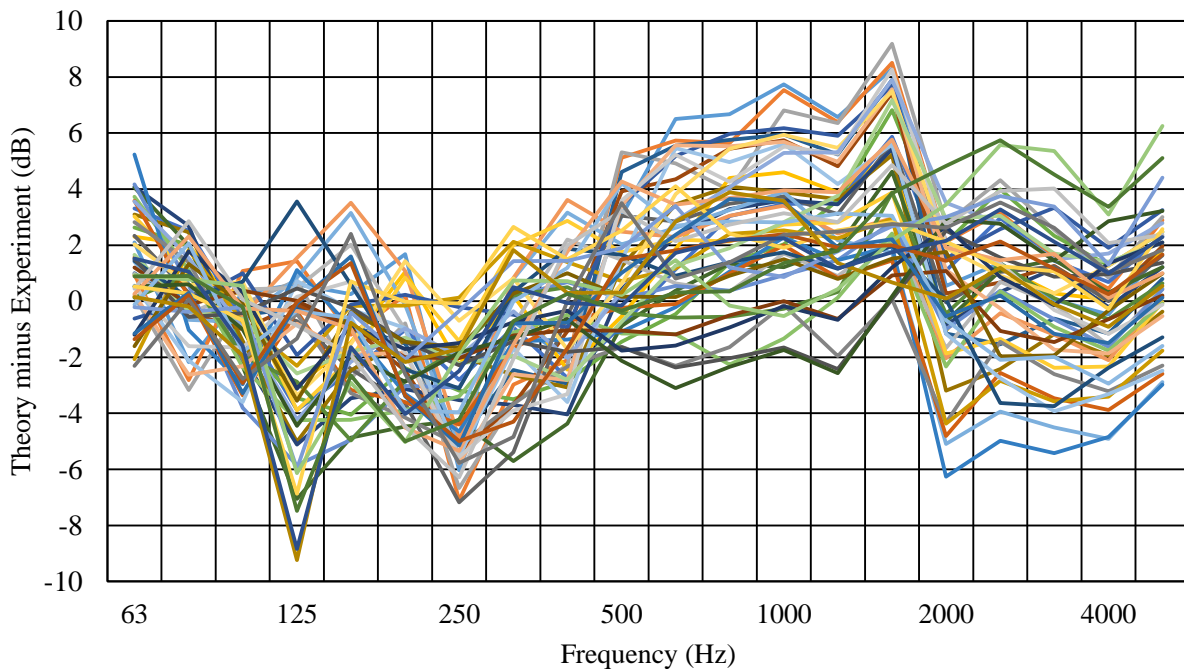
401
 402 Table VI gives the same information for 8 cavity walls, with 39 x 89 mm wood studs and
 403 layers of 13 or 16 mm gypsum plaster board (GPB) on each side, measuring 3.05 m wide by 2.44
 404 m high. The numbers in the GPB Layers columns denote the thicknesses of the GPB layers in mm.

405 The letter X denotes type X fire rated GPB. The wood stud wall data is taken from Halliwell et al.
406 (1998) and experimentally determined values of Young's modulus and surface density were used.
407 Quirt *et al.* (1995) determined the Young's modulus by supporting beams of gypsum plaster board
408 horizontally on pipe supports with a 2.5 cm overhang at both ends. The beams were tapped with
409 an impact hammer or a finger and the impulse response at the centre of the beam was measured
410 with an accelerometer. The impulse response was Fourier transformed to obtain the frequency
411 response. The frequency of the first beam mode was determined from the first resonance frequency
412 peak in the frequency response and the Young's modulus was calculated by assuming that the
413 beam was simply supported.



414
415 FIG. 3. (Color online) The difference in sound insulation between the theoretical prediction
416 using the line connection model and the experimental measurement for 92 mm steel stud cavity
417 walls, with layers of 16 mm gypsum plaster board on each side.

418 For the six 16 gauge steel stud walls with a height of 4.57 m, multiplying the simply
419 supported resonance frequency by an frequency multiplier r of 1.7 worked well. This frequency
420 multiplier r was also good for the higher walls with 18 gauge and equivalent 20 gauge studs spaced
421 at 610 mm with two layers of 16 mm GPB on each side or with two layers on one side and one
422 layer on the other side. The other 18 gauge and equivalent 20 gauge stud walls needed a frequency
423 multiplier r of only 1.3. Frequency multipliers r of 1.7 and 1.3 were used for the higher 20 gauge
424 stud walls with stud spacings of 610 mm and 406 mm respectively. The higher 25 gauge stud walls
425 needed a frequency multiplier r of only 1.



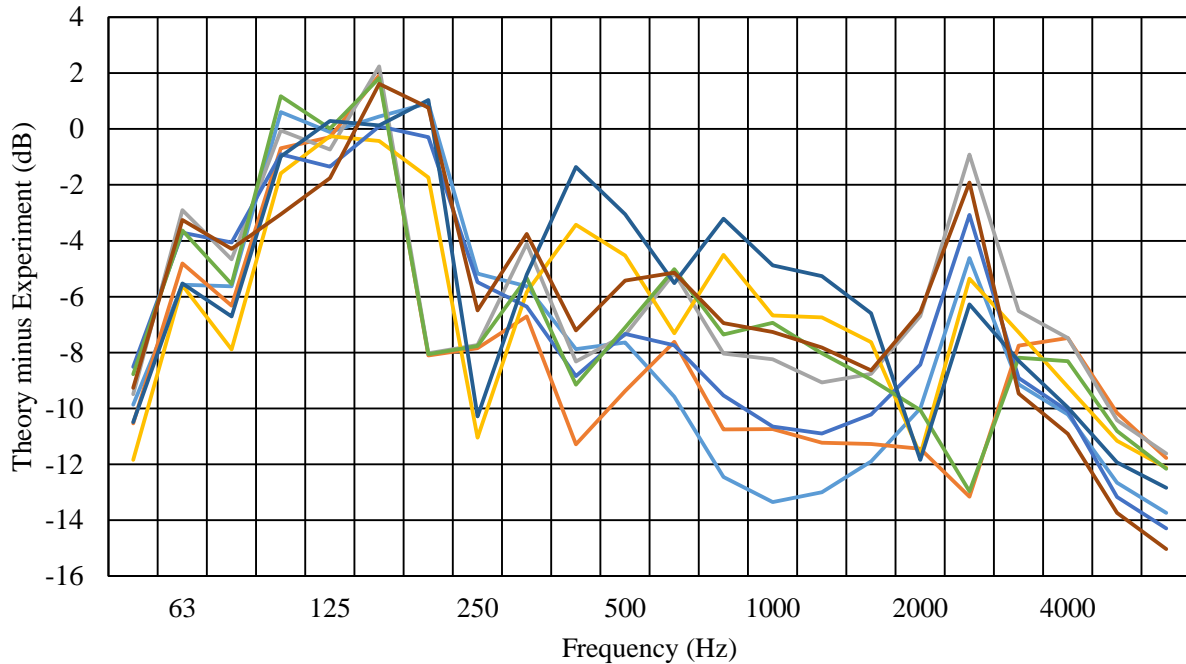
426
427 FIG. 4. (Color online) The difference in sound insulation between the theoretical prediction
428 using the point connection model and the experimental measurement for 92 mm steel stud cavity
429 walls, with layers of 16 mm gypsum plaster board on each side.

430 A frequency multiplier r of 1.3 was used for the lower height 16 and 20 gauge stud walls
431 except for the two walls with a stud spacing of 610 mm and two layers of GPB on each side of the

432 studs which both used a frequency multiplier r of 1.7. The lower height 25 gauge stud walls needed
433 a frequency multiplier r of 0.6 except for the wall with a stud spacing of 406 mm and two layers
434 of GPB on each side which required a frequency multiplier of 0.8. Thus, the general trend was for
435 the frequency multiplier r to decrease as the stud gauge increased, as the reduced mass decreased
436 and as the stud spacing decreased. It is interesting to note that for the resonance frequencies of
437 concrete floor slabs, Japanese researchers (Masuda and Tanaka, 2018) use the approximate
438 formula for the resonance frequencies for a clamped panel with a frequency multiplier of 0.8. This
439 is the same as a frequency multiplier of 1.8 times the simply supported panel resonance
440 frequencies.

441 For the eight wooden stud walls, the frequency multiplier r varied between 1.4 and 1.9 with
442 no obvious pattern, although the frequency multiplier r was 1.7 for half of the walls. For these
443 wooden stud walls the absorption multiplier B was 0.3 for seven of the walls and 0.2 for the other
444 wall. The maximum frequency of application f_B of the absorption multiplier was 160 Hz for five
445 of the walls and 125 Hz for the three other walls. There was a tendency for the walls with the
446 highest reduced mass to have the higher maximum frequency of application.

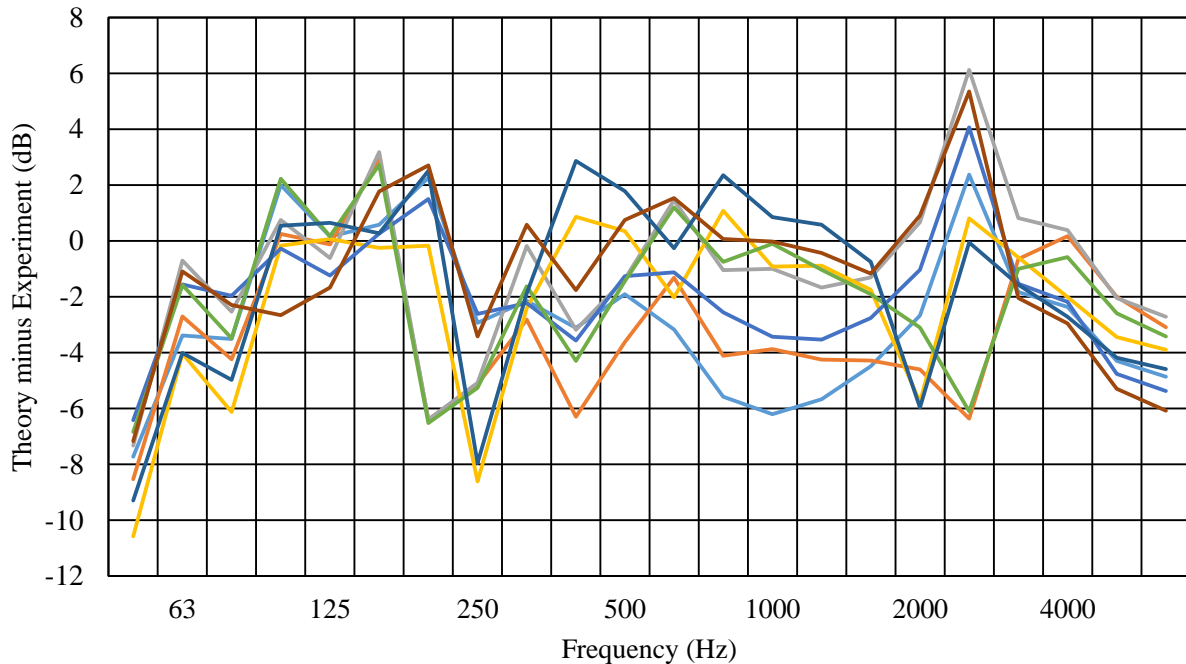
447 For the steel stud walls, the absorption multiplier B varied between 0.4 and 1 except for
448 one value B of 0.15. The absorption multiplier B was different from 1 for all but one of the lower
449 height walls. For the higher steel stud walls, the absorption multiplier B was different from 1 for
450 the 16, 18 and 20 gauge walls with a stud spacing of 406 mm and the maximum frequency of
451 application f_B was 160 Hz for these walls. The situation was reversed for the higher height 25
452 gauge steel stud walls and the absorption multipliers B were different from 1 for the 610 mm stud
453 spacings and the maximum frequency of application f_B was 80 Hz for the two heavier walls and
454 63 Hz for the lighter wall.



455

456 FIG. 5. (Color online) The difference in sound insulation between the theoretical prediction
 457 using the line connection model and the experimental measurement for 39 x 89 mm wood stud
 458 cavity walls, with layers of 13 or 16 mm gypsum plaster board on each side.

459 FIG. 3 and FIG. 4 show the differences between the predicted sound insulation and the
 460 experimentally measured sound insulation for the line compliance model and the point compliance
 461 model respectively for the steel stud walls. The point compliance model gives slightly more spread
 462 of differences than the line compliance model. The spread of differences at and above the critical
 463 frequency is believed to be because the different walls have a range of in situ damping loss factor
 464 values compared to the value of 0.03 assumed in this paper.



465

466 FIG. 6. (Color online) The difference in sound insulation between the theoretical prediction
 467 using the point connection model and the experimental measurement for 39 x 89 mm wood stud
 468 cavity walls, with layers of 13 or 16 mm gypsum plaster board on each side.

469 FIG. 5 and FIG. 6 show the differences between the predicted sound insulation and the
 470 experimentally measured sound insulation for the line compliance model and the point compliance
 471 model respectively for the wood stud walls. FIG. 5 shows, as Davy (2012) commented, that above
 472 200 Hz the line connection model underestimates the sound insulation of the wood stud building
 473 elements. Presumably a similar under prediction would occur for steel stud building elements if
 474 the empirically determined line compliance did not automatically include a correction for this
 475 difference because of the way it was derived. Applying the empirical corrections presented in this
 476 paper has led to the under prediction of the sound insulation of the wood stud building elements in
 477 the frequency range below 100 Hz.

478 There are still large differences between theory and experiment at some frequencies. One
479 of the reasons for this is the very rapid increase in the experimental sound insulation immediately
480 above the effective normal incident mass-air-mass resonance frequency, which the simple theory
481 used in this paper cannot reproduce. Another reason is the very rapid decrease in the experimental
482 sound insulation as the critical frequency is approached from below. Again, simple sound
483 insulation theories cannot predict this rapid decrease.

484 There is also a big variation in the difference between theory and experiment above the
485 critical frequency. This is believed to be due to a large variation in the in-situ damping loss factor
486 between different building element specimens compared to the value of 0.03 assumed in this paper,
487 although on average the 0.03 value for the damping loss factor appears to be correct.

488 **V. CONCLUSION**

489 This paper presents the theory for calculating the effective normal incident mass-air-mass
490 resonance frequency for a double leaf cavity stud building element. If the two building element
491 leaves are similar, this frequency is the root mean square of the first bending wave mode resonance
492 frequency of the building element leaf between adjacent studs and the normal incident mass-air-
493 mass resonance frequency of the version of the building element without studs. If the building
494 element cavity contains porous sound absorbing material, the isothermal normal incident mass-
495 air-mass resonance frequency should be used. Although not shown in this paper, for a building
496 element cavity without porous sound absorbing material, it is expected that the adiabatic normal
497 incident mass-air-mass resonance frequency should be used.

498 Because the exact boundary conditions of the building element leaves at the studs are not
499 known, and because these boundary conditions will depend on the compliance of the studs, this

500 paper gives empirically determined factors by which to multiply the first bending wave mode
501 resonance frequency of the building element leaf between adjacent studs with simply supported
502 boundary conditions in order to obtain this resonance frequency with the actual boundary
503 conditions.

504 In order to calculate the correct sound insulation of a double leaf cavity stud building
505 element with porous sound absorbing material in its cavity in the vicinity of the effective normal
506 incident mass-air-mass resonance frequency, this paper gives empirically determined factors by
507 which the assumed sound absorption coefficient of the cavity must be multiplied and the
508 empirically determined frequency up to and including which this multiplication factor must be
509 used.

510 This paper also gives empirically derived equations for the equivalent translational line and
511 point compliances of steel studs manufactured from different sheet steel gauges. It compares these
512 equations for the case of 25 gauge steel studs with earlier research.

513 The range of differences between theory and experiment for the sound insulation of cavity
514 stud building elements with porous sound absorbing material in their cavities have been
515 significantly reduced in the region of the effective normal incident mass-air-mass resonance
516 frequency but is still large across the whole frequency range.

517 **REFERENCES**

518 B  tit, A. (2010). "Performance details of metal stud partitions," *Sound and Vibration* **March**
519 **2010**, 14-16.

520 Bradley, J. S. (2002). "IBANA-Calc Validation Studies," in *Institute for Research in*
521 *Construction Research Report IRC RR-125* (National Research Council of Canada), p.

522 50.

523 Bradley, J. S., and Birta, J. A. (2000). "Laboratory measurements of the sound insulation of
524 building façade elements," in *Institute for Research in Construction Internal Report IRC*
525 *IR-818* (National Research Council of Canada, Ottawa), p. 183.

526 Bradley, J. S., and Birta, J. A. (2001). "On the sound insulation of wood stud exterior walls," *J.*
527 *Acoust. Soc. Am.* **110**, 3086-3096.

528 Bradley, J. S., Lay, K., and Norcross, S. G. (2002). "Measurements of the sound insulation of a
529 wood framed house exposed to aircraft noise," in *Institute for Research in Construction*
530 *Internal Report IRC IR-831* (National Research Council of Canada, Ottawa), p. 113.

531 Cremer, L. (1942). "Theorie der Schalldämmung Wände bei schrägem Einfall, Akustische,"
532 *Zeitschrift* **7**, 81–104.

533 Davy, J. L. (2009). "Predicting the sound insulation of walls," *Build. Acoust.* **16**, 1-20.

534 Davy, J. L. (2010). "The improvement of a simple theoretical model for the prediction of the
535 sound insulation of double leaf walls," *J. Acoust. Soc. Am.* **127**, 841-849.

536 Davy, J. L. (2012). "Sound transmission of cavity walls due to structure borne transmission via
537 point and line connections," *J. Acoust. Soc. Am.* **132**, 814–821.

538 Davy, J. L., Debevc, M., and Blanc, C. (2017). "The sound insulation autoclaved aerated
539 concrete panels lined with gypsum plaster board," in *Inter-noise 2017* (I-INCE, Hong
540 Kong, China), pp. 3879-3889.

541 Davy, J. L., Fard, M., Dong, W., and LoVerde, J. (2018). "The equivalent translational
542 compliance of steel studs with different steel gauge thicknesses," in *Inter-noise 2018*
543 (Chicago, USA), p. 12.

544 Davy, J. L., Guigou-Carter, C., and Villot, M. (2012). "An empirical model for the equivalent

545 translational compliance of steel studs," *J. Acoust. Soc. Am.* **131**, 4615–4624.

546 Dong, W., and Loverde, J. (2015). "Analysis of the effects on transmission loss of changes to
547 stud gauge, spacing, and height in single steel stud walls," in *Inter-noise 2015* (INCE
548 USA, San Francisco, USA), p. 10.

549 Halliwell, R. E., Nightingale, T. R. T., Warnock, A. C. C., and Birta, J. A. (1998). "Gypsum
550 board walls: transmission loss data," in *Internal Report IRC-IR-761* (Institute for
551 Research in Construction, National Research Council of Canada, Ottawa, Canada), p.
552 370.

553 Heckl, M. (1959a). "Shallabstrahlung von Platten bei Punktförmiger Anregung (Sound radiation
554 of plates with point excitation)," *Acustica* **9**, 371-380.

555 Heckl, M. (1959b). "Untersuchungen über die Luftschalldämmung von Doppelwänden mit
556 Schallbrücken (Investigations on the airborne sound insulation of double walls with
557 sound bridges)," in *The Third International Congress on Acoustics*, edited by L. Cremer
558 (Elsevier Publishing Company, Stuttgart, Germany), pp. 1010-1014.

559 Hirakawa, S., and Davy, J. L. (2015). "The equivalent translational compliance of steel or wood
560 studs and resilient channel bars," *J. Acoust. Soc. Am.* **137**, 1647-1657.

561 Lin, G. F., and Garrelick, J. M. (1977). "Sound-transmission through periodically framed parallel
562 plates," *J. Acoust. Soc. Am.* **61**, 1014-1018.

563 Loverde, J., Dong, W., and Bétit, A. (2012). "Investigation into the acoustical performance of
564 single stud steel wall assemblies," in *Internoise 2012* (New York City, USA), p. 6.

565 Masuda, K., and Tanaka, H. (2018). "Prediction of heavy impact sound level using mode shape
566 function method," in *25th International Congress on Sound and Vibration* (International
567 Institute of Sound and Vibration, Hiroshima, Japan), pp. 1-8.

568 Mulholland, K. A., Parbrook, H. D., and Cummings, A. (1967). "The Transmission Loss of
569 Double Panels," *Journal of Sound and Vibration* **6**, 324–334.

570 Narang, P. P. (1993). "Effect of fiberglass density and flow resistance on sound transmission loss
571 of cavity plasterboard walls," *Noise Control Engineering Journal* **40**, 215-220.

572 Nash, A. (2006). "Resilient ceiling construction in residential buildings," in *4th Joint ASA/ASJ*
573 *Meeting (152nd Meeting of ASA)* (Honolulu HI USA), pp. 1-15.

574 Nightingale, T. R. T., and Bosmans, I. (1999). "Vibration response of lightweight wood frame
575 building elements," *Build. Acoust.* **6**, 289-308.

576 Poblet-Puig, J., Rodriguez-Ferran, A., Guigou-Carter, C., and Villot, M. (2009). "The role of
577 studs in the sound transmission of double walls," *Acta Acust. Acust.* **95**, 555-567.

578 Quirt, J. D., Warnock, A. C. C., and Birta, J. A. (1995). "Sound transmission through gypsum
579 board walls: Sound transmission results," in *Internal Report IRC-IR-693* (National
580 Research Council of Canada, Ottawa, Canada), p. 83.

581 Rudder, F. F. J. (1985). "Airborne Sound Transmission Loss Characteristics of Wood-Frame
582 Construction, General Technical Report, FPL-43," (Forest Products Laboratory, Forest
583 Service, United States Department of Agriculture, Madison, Wisconsin, USA), pp. 1-27.

584 Sewell, E. C. (1970). "Transmission of Reverberant Sound through a Single-Leaf Partition
585 Surrounded by an Infinite Rigid Baffle," *J.Sound Vib.* **12**, 21–32.

586 Sharp, B. H. (1973). "A study of techniques to increase the sound insulation of building
587 elements," in *Wyle Laboratories Report WR 73-5, Wyle Laboratories Research Staff, El*
588 *Segundo, California, distributed as PB-222 829, National Technical Information Service,*
589 *United States Department of Commerce, Springfield, Virginia.,* pp. 1-227.

590 Sharp, B. H. (1978). "Prediction Methods for the Sound Transmission of Building Elements,"

591 Noise Control Eng. **11**, 53-63.

592 Sharp, B. H., Kasper, P. K., and Montroll, M. L. (1980). "Sound Transmission through Building
593 Structures - Review and Recommendations for Research," in *NBS-GCR-80-250, National*
594 *Bureau of Standards, United States Department of Commerce, Washington, D. C., .*
595 *Distributed as PB81-187072, National Technical Information Service, United States*
596 *Department of Commerce, Springfield, Virginia, pp. 1-144.*

597 Van den Wyngaert, J. C. E., Schevenels, M., and Reynders, E. P. B. (2018). "Predicting the
598 sound insulation of finite double-leaf walls with a flexible frame," *Appl. Acoust.* **141**, 93-
599 105.

600 Vigran, T. E. (2010a). "Sound insulation of double-leaf walls - allowing for studs of finite
601 stiffness in the transfer matrix scheme," *Appl. Acoust.* **71**, 616-621.

602 Vigran, T. E. (2010b). "Sound transmission in multilayered structures - Introducing finite
603 structural connections in the transfer matrix method," *Appl. Acoust.* **71**, 39-44.

604